Advancing Water-Enhanced Direct Air Capture of Carbon Dioxide with Multi-Step Amine Functionalized Metal-Organic Frameworks

Oscar Iu-Fan Chen, Omar M. Yaghi

ABSTRACT: In this work, we have developed two distinct amine-functionalization series for a zirconium-based metal-organic framework (MOF), MOF-808. These strategies involved the direct coordination of amino acids with zirconium metal ions and the covalent incorporation of polyamines The MOF variants underwent thorough characterization and testing for their suitability in direct air capture (DAC) of CO₂. Multiple analytical techniques, encompassing liquid-state ¹H nuclear magnetic resonance (NMR) measurements, potentiometric acid-base titration, and with energy-dispersive X-ray spectroscopy was comprehensively employed to assess the loading quantity of the amine functionalities. Following amine functionalization, improved CO₂ capture performance was investigated using single-component sorption isotherms and dynamic breakthrough measurements. In dry conditions, the L-lysine- and tris(3-aminopropyl)amine-functionalized variants, termed as MOF-808-Lys and MOF-808-TAPA, exhibited the highest CO₂ uptakes at 400 ppm, measuring 0.612 and 0.498 mmol g⁻¹. Further capacity enhancement was achieved by introducing 50% relative humidity, resulting in a remarkable 97% and 75% increase compared to the dry uptakes, respectively. The enhanced uptake efficiency was demonstrated by ¹³C solid-state NMR, revealing the formation of bicarbonate species. This research indicates a broader potential for advancing MOF materials through judicious post-synthetic amine functionalization for DAC applications.

Introduction

The fast-paced development of industry and technology has led to a significant increase in energy demands, heavily reliant on the combustion of fossil fuels, which has resulted in the emission of substantial amounts of carbon dioxide (CO₂), contributing to severe environmental issues1. In light of this, a crucial solution to combat CO2 emissions from the atmosphere is through the implementation of direct air capture (DAC)²⁻⁴. To effectively capture CO₂ from the ambient air, which is present at a low concentration (0.04%), it is essential to have highly reactive specific sites for CO₂ adsorption. In this context, amine functionalities have emerged as promising candidates for chemisorption sites, facilitating the development of efficient CO₂ capture sorbents⁵⁻¹¹. While current methods involve using aqueous alkaline solutions^{12, 13} to chemically bind CO2, they suffer from significant drawbacks such as energy-intensive desorption processes and poor long-term cyclability. These issues result in high energy consumption and unavoidable secondary CO2 emissions, leading to elevated costs. Therefore, it is imperative to develop protocols that exhibit high CO₂ capacity, low energy penalty, and exceptional chemical stability for the DAC scenarios, as they hold the key to effectively addressing this challenge.

Numerous categories of solid-state materials have undergone extensive exploration to fulfill the criteria for efficient CO₂ sorbents and to decipher the CO₂ sorption chemistry, including zeolites^{5, 14}, polymers^{8, 15, 16}, silicas^{10, 17-19}, metal-organic frameworks (MOFs)^{7, 20-26}, and covalent

organic frameworks (COFs)9, 27. In our prior research endeavors²⁸, we formulated and synthesized a sequence of coordinatively amino acid-functionalized materials, termed MOF-808-AAs (AAs = amino acids), with the primary aim of elucidating the mechanism underlying CO₂ capture via amine moieties. We thus observed the favorable amine-CO2 interaction attributed to the generation of bicarbonate species^{28, 29} facilitated by water vapor. Expanding upon this foundational understanding, our current investigations have led us to develop a novel series of postsynthetically functionalized MOF-808 materials, designated as MOF-808-PAs (PAs = polyamines), involving the covalent incorporation of 4 different liquid polyamines via two-step functionalization. Combined with 4 meticulously optimized or newly synthesized MOF-808-AA materials, the composition, porosity, and inherent pore characteristics of these compounds have been fully characterized. Furthermore, their performance in CO₂ uptake under both dry and humid conditions has also been evaluated, encompassing aspects such as sorption capacity, adsorption and desorption behavior, and overall cycling proficiency. Notably, the phenomenon of water-enhanced CO₂ capacities can be observed through the dynamic breakthrough measurements, offering a valuable blueprint for the strategic advancement of CO₂ sorbents tailored for DAC applications.

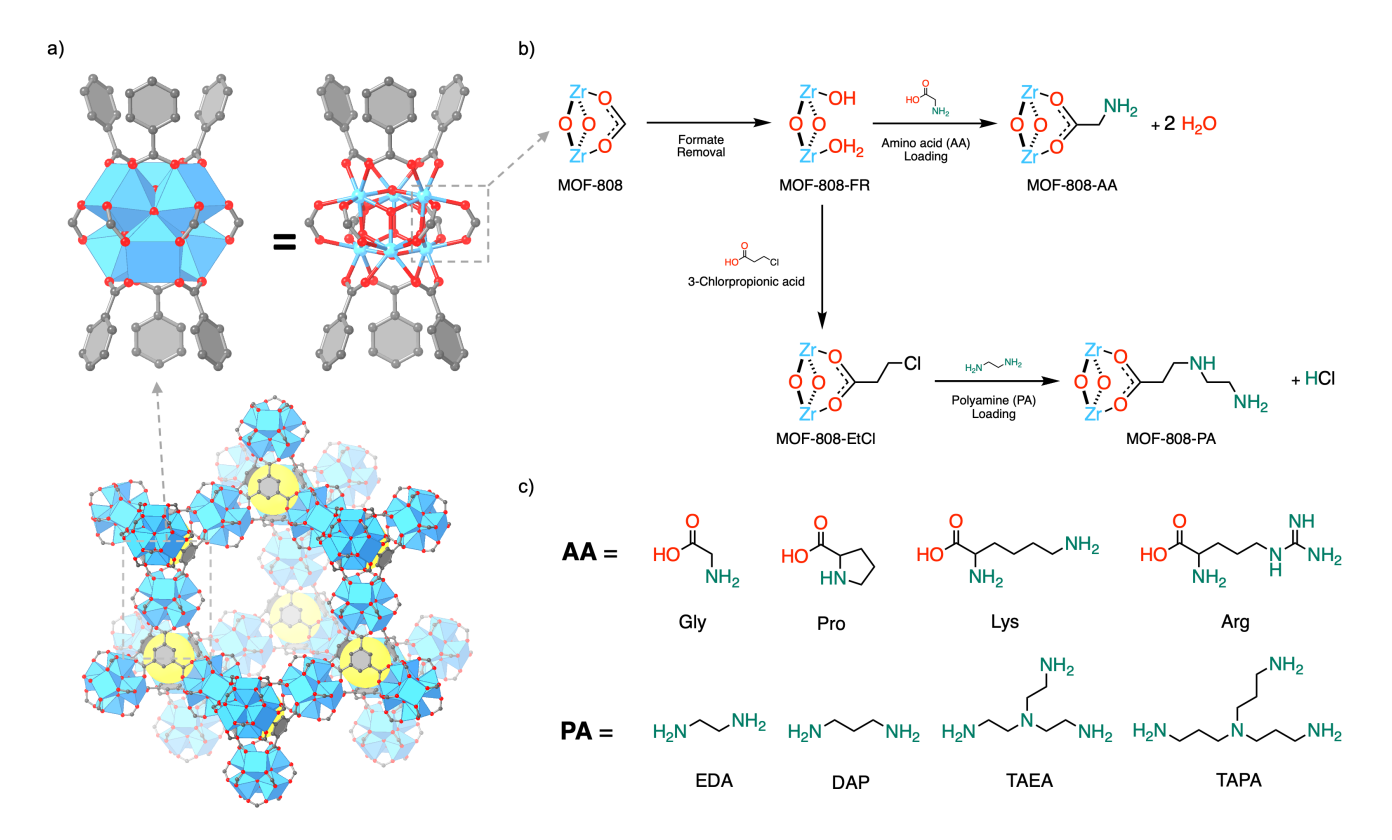


Figure 1. (a) Structure of MOF-808 and (b) general synthetic scheme for MOF-808-AA and MOF-808-PA. Selected installed amino acids and polyamines are provided in (c). Zr atoms are represented as light blue polyhedra, while other atoms are represented as spheres (color code: C, gray; O, red). H atoms are omitted, and the yellow spheres highlight the small tetrahedral pores for clarity.

Design and synthesis

Due to its remarkable robustness³⁰⁻³², efficient large-scale preparatory process³³, and capacity for post-synthetic modifications³⁴⁻³⁷, MOF-808 [Zr₆O₄(OH)₄(BTC)₂(HCOO)₆, BTC = 1,3,5-benzenetricarboxylate] (Figure 1a) was chosen as the foundational material for amine-functionalization and was synthesized following previously established procedures²⁸. Subsequently, MOF-808-FR was derived through the elimination of formate ligands via hydrochloric acid (HCl) treatment at 85 °C for a duration of 5 days. The targeted functionalities were then introduced onto the MOF-808 backbones through the coordination between Zr(IV) and carboxylate groups, thereby fine-tuning the pore environment and creating specific chemisorption sites tailored for CO₂ capture.

For the preparation of MOF-808-AA sorbents (Figure 1b), termed as MOF-808-Gly, MOF-808-Pro, MOF-808-Lys, and MOF-808-Arg, 4 amino acids (Figure 1c), namely glycine, DL-proline, L-lysine, and L-arginine, were selected with their high pKa of the amines38 to provide strong chemical interaction with CO₂. The MOF-808-FR powder was immersed in saturated solutions of these amino acids for a duration of 1 to 3 days at the designated temperature. The resultant solid was then collected, subjected to washing with deionized water and acetone, followed by treatment with a 10% solution of 1,8diazabicyclo[5.4.0]undec-7-ene (DBU) in tetrahydrofuran (THF) to achieve amine deprotonation and hydrochloride salt removal. Further activation was performed using dynamic vacuum conditions, resulting in the creation of MOF-808-AA samples. In pursuit of enhancing the loading capacity of amino acids and achieving a greater density of chemisorption sites, an extensive screening process has been conducted to assess the optimal loading solvent, temperature, and reaction duration within the synthetic procedure. In order to prevent the potential degradation of MOF-808 during the loading procedure at elevated temperatures caused by the strong basic nature of L-lysine and L-arginine, their hydrochloride salt forms were employed. Moreover, it was determined that ethylene glycol exhibited remarkable solubility and superior loading capabilities for these two amino acid species. This significant finding contributed to a substantial enhancement in loading efficiency, effectively reducing both reaction time and solvent usage.

On the other hand, a two-step polyamine-functionalization strategy has been devised to develop the MOF-808-PA series (Figure 1b). Initially, 3-chloropropionic acid was introduced by binding its carboxylate groups to Zr(IV) of MOF-808 coordinatively. Parallel to the synthetic procedure implemented for the MOF-808-AA series, the process began by immersing MOF-808-FR powder in a saturated aqueous solution of 3chloropropionic acid at 85°C, with the solution being freshly replenished within a 3-day interval. After the solvent exchange and activation process, it yielded the formation of MOF-808-EtCl, serving as the foundation for the following step. Subsequently, the newly synthesized product was treated with the polyamine solutions at 85°C for 24 hours. Four distinct polyamines (Figure 1c), ethylenediamine (EDA), 1,3-diaminopropane (DAP), tris(3-aminoethyl)amine (TAEA), and tris(3-aminopropyl)amine (TAPA), were utilized for this amine-functionalization. The covalent incorporation of selected polyamines was executed through nucleophilic substitution, replacing chloride ions of the installed 3-chloropropionic acid. The resultant solid was then collected, subjected to washing, and activated, ultimately yielding MOF-808-PA products. (termed as MOF-808-EDA, MOF-808-DAP, MOF-808-TAEA, and MOF-808-TAPA). This strategic approach notably enhanced the density of accessible sorption sites, with a particularly pronounced effect observed with TAEA and TAPA, effectively doubling the count of primary amine groups per loaded molecule, ultimately contributing to inced CO₂ uptake capabilities.

The composition of the functionalized MOF-808 samples was comprehensively determined through an array of analytical techniques, encompassing liquid-state ¹H nuclear magnetic resonance (NMR) measurements, potentiometric acidbase titration, and scanning electron microscopy (SEM) with energy-dispersive X-ray spectroscopy (EDS). To further characterize the samples, nitrogen sorption isotherm and powder X-ray diffraction (PXRD) analyses were employed to investigate their porosity and crystallinity. Additionally, water vapor isotherm measurements were conducted to explore the influence of water during CO₂ capture. To delve into the CO₂ uptake performance under distinct conditions, both CO₂ sorption isotherm and dynamic breakthrough measurements were undertaken. These investigations aimed to shed light on the samples' performance at DAC conditions, in dry environments or in the presence of water. Furthermore, the desorption behavior and cycling performance were evaluated to gauge the efficiency and stability of the functionalized MOF-808 materials. Finally, solid-state NMR was employed to decipher the chemisorption mechanism of amine functional groups and CO₂.

Structural and compositional characterization

The retention of crystallinity across all modified MOF-808 variants was evident in the PXRD measurements (Section S5). In comparison with the simulated PXRD pattern of MOF-808, there have been no noticeable phase changes or degradation observed in the MOF-808-AA series following the post-synthetic functionalization process. For the MOF-808-PA series, some minor degradation was observed, which was likely linked to the disorder introduced by incorporating polyamine molecules into the MOF structure. This outcome underscored the resilience of MOF-808, solidifying its potential as a robust platform for targeted applications through post-synthetic modification.

To assess the loading quantity of the designated molecules, the activated functionalized MOF samples were fully hydrolyzed with the aid of hydrofluoric acid (HF) and deuterium chloride (DCl) within a solvent mixture of DMSO- d_6 and deuterium oxide (D2O). The identification of the loaded molecules was achieved through the introduction of minute quantities of pure molecules into the MOF samples, which were subsequently subjected to analysis via digest NMR (Section S3). The distinct peaks attributable to the targeted molecules within the resulting spectra were discernible through increased integration. Upon this analytical framework, the loading numbers of amino acids per secondary building unit (SBU) of MOF-808-Gly and MOF-808-Pro were quantified as 4.19 and 3.90 (Figure S3-4), respectively. These values translated to a gravimetric effective amine loading of 3.28 and 2.05 mmol g-1. For MOF-808-Lys and MOF-808-Arg, the established loading numbers were 2.81 and 2.77 (Figure S5-6), which correspond to a gravimetric primary amine loading of 3.98 and 3.28 mmol g⁻¹. As a result, MOF-808-Lys emerged as the exemplar within the series, boasting the highest effective amine loading.

On the contrary, quantifying the loaded polyamine content using digest NMR presents a considerable challenge due to potential change in chemical shifts following covalent incorporation. Thus, the utilization of potentiometric acid-base titration³⁹ (Section S4) served as a viable alternative to evaluate the amount of basic components within the MOF-808-PA series—specifically, the amine functionalities, which also allowed for the assessment of functionalized polyamine quantities. In this method, the MOF samples were ground and suspended in an aqueous NaNO₃ solution. The pH of the solution was adjusted to a range of 10-11 using a 0.1 M aqueous NaOH solution prior to the titration process, which was carried out by adding 0.1 M aqueous HCl solution incrementally. It is worth noting that two distinct equivalence points manifested across the titration curves for all MOF-808-PA samples. These points signified the presence of unreacted primary amines and the secondary amines, each possessing a different level of basicity. The pKa values were calculated accordingly at 9.4 - 9.8 and 10.2 - 10.3 for two equivalent points (Table S1), respectively, and the loaded polyamines were also quantified in a range from 1.61 to 2.05 mmol g⁻¹ of MOF-808-PA series (Figure S12-15, Table S3). The TAPA variant demonstrated the highest conversion rate (98.1%) based on the loading of 3-chloropropionic acid with a value of 2.07 mmol g⁻¹ using digestion NMR (Figure S7), and this was accompanied by the highest gravimetric primary amine loading, reaching 4.10 mmol g⁻¹. Additionally, the potentiometric acid-base titration method was also employed to ascertain the loading of amino acids within the MOF-808-AA series (Figure S8-11. Table S2). For MOF-808-Lys and MOF-808-Arg, two equivalence points can be observed, indicating the number of the basic functionality. Remarkably, the results obtained from this titration process aligned closely with values acquired through digestion NMR (Figure 2). The great agreement exhibited the reliability of the analytical procedure, furnishing an invaluable strategy for the evaluation of active sites for CO₂ capture applications.

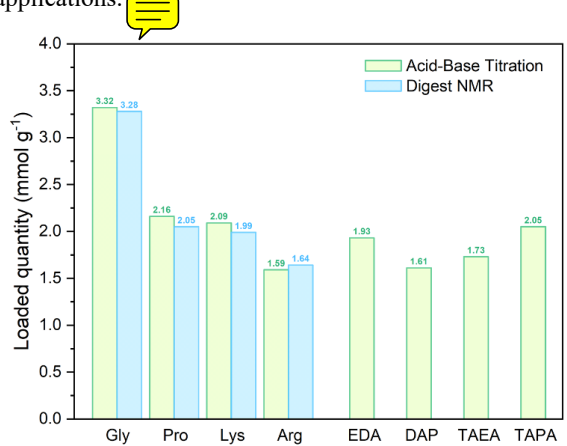


Figure 2. Comparison of loaded amino acids/polyamines in MOF-808-AA and MOF-808-PA series by employing acid-base titration (light green) and ¹H digest NMR (light blue).

The effectiveness of the two-step post-synthetic functionalization process for the MOF-808-PA series was validated through SEM-EDS measurements (Section S6). In the pristine MOF-808 sample, no signals associated with Cl or N were detected. Upon introducing 3-chloropropionic acid, the MOF-

808-EtCl sample exhibited a noticeable Cl signal, confirming the successful molecule installation. Following the subsequent polyamine functionalization step, a reduction in Cl signal intensity was observed, accompanied by an increase in N signal intensity. These observations pointed to the elimination of Cl atoms via nucleophilic substitution and the incorporation of the polyamines. This analysis thus reinforced the affirmation of the successful functionalization process within the MOF-808-PA series.

Nitrogen and water sorption isotherms

Nitrogen sorption isotherms were measured at a temperature of 77 K to investigate the permanent porosity and poresize distribution of different variants of MOF-808 (Figure 3, Section S7). The comparison between MOF-808 and MOF-808-FR showed that the nitrogen uptake increased after the removal of formate ligands, associated with a slight rise in the calculated Brunauer-Emmett-Teller (BET) surface area from 1545 to 1610 m² g⁻¹. This phenomenon can be explained by the elimination of formate ligands, which resulted in a larger effective volume. In contrast, when examining the MOF-808-AA series, the introduction of amino acids led to a decrease in nitrogen sorption capacities, resulting in both lower BET surface areas (ranging from 573 to 1361 m² g⁻¹) and pore sizes (ranging from 8.5 to 14.9 Å). This decrease was attributed to factors such as the loading number and the molecular size of the amino acids. In the case of the MOF-808-PA series, the nitrogen sorption capacities also decreased following the incorporation of polyamines and can be translated into BET surface areas ranging from 321 to 676 m² g⁻¹. One significant observation was the presence of a typical type H3 hysteresis loop⁴⁰ during the desorption process for all four samples, which occurred in the pressure range between $P/P_0=0.5$ and 1.0, usually found on the material with wide pore size distributions. This observation was further supported by the calculated specific pore volumes and pore sizes, which exhibited two distinct values, pointing to the uneven distribution of polyamine incorporation. Particularly, the pore size of MOF-808-EtCl closely resembled that of the larger pores within the MOF-808-PA series, indicative of the distribution of unreacted 3-chloropropionic acid. Conversely, the smaller pores represented the areas of concentrated amine functionalities.

To explore the effects of post-synthetically incorporated functionalities on the pore environment, water sorption isotherms were conducted at 298 K (Figure 3, Section S8). In the case of MOF-808, a distinct steep pore-filling step occurred at approximately 35% relative humidity (RH), accompanied by an adsorption capacity of 0.3 g g-1. Following the removal of formate groups, water adsorption commenced at lower RH levels and demonstrates a significantly increased total adsorption capacity of 0.55 g g⁻¹. This enhancement was attributed to the direct interaction between water molecules and the hydrophilic zirconium nodes within the structure. The introduction of amino acids into the MOF-808-AA series similarly resulted in an early onset of water sorption at lower RH levels. However, the overall uptake capacity diminished notably when compared to the original MOF-808. Within the MOF-808-PA series, a hysteresis phenomenon was also observed in the water sorption behavior. In summary, all variants of MOF-808 exhibited great affinity for water molecules, indicating a conducive environment for robust interactions with CO₂.

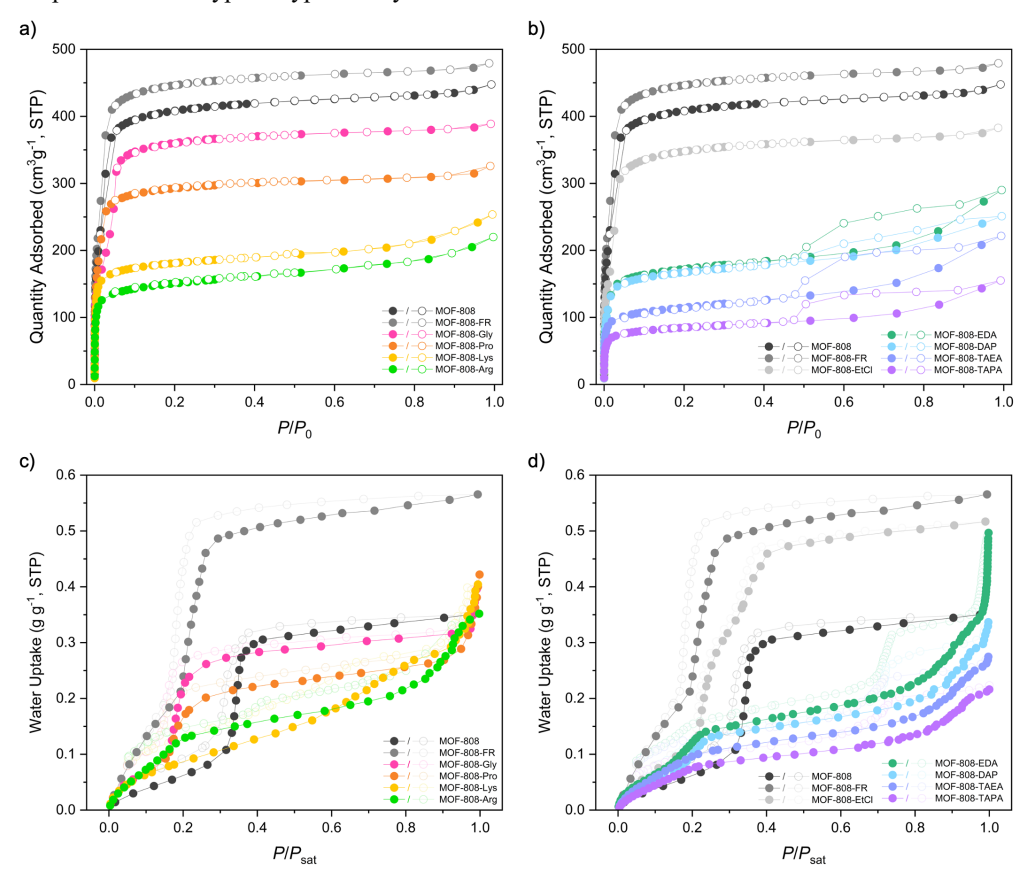


Figure 3. Comparison of (a)(b) N_2 sorption isotherms at 77 K and (c)(d) water sorption isotherms at 25 °C of MOF-808, MOF-808-FR, MOF-808-EtCl, MOF-808-AAs, and MOF-808-PAs .

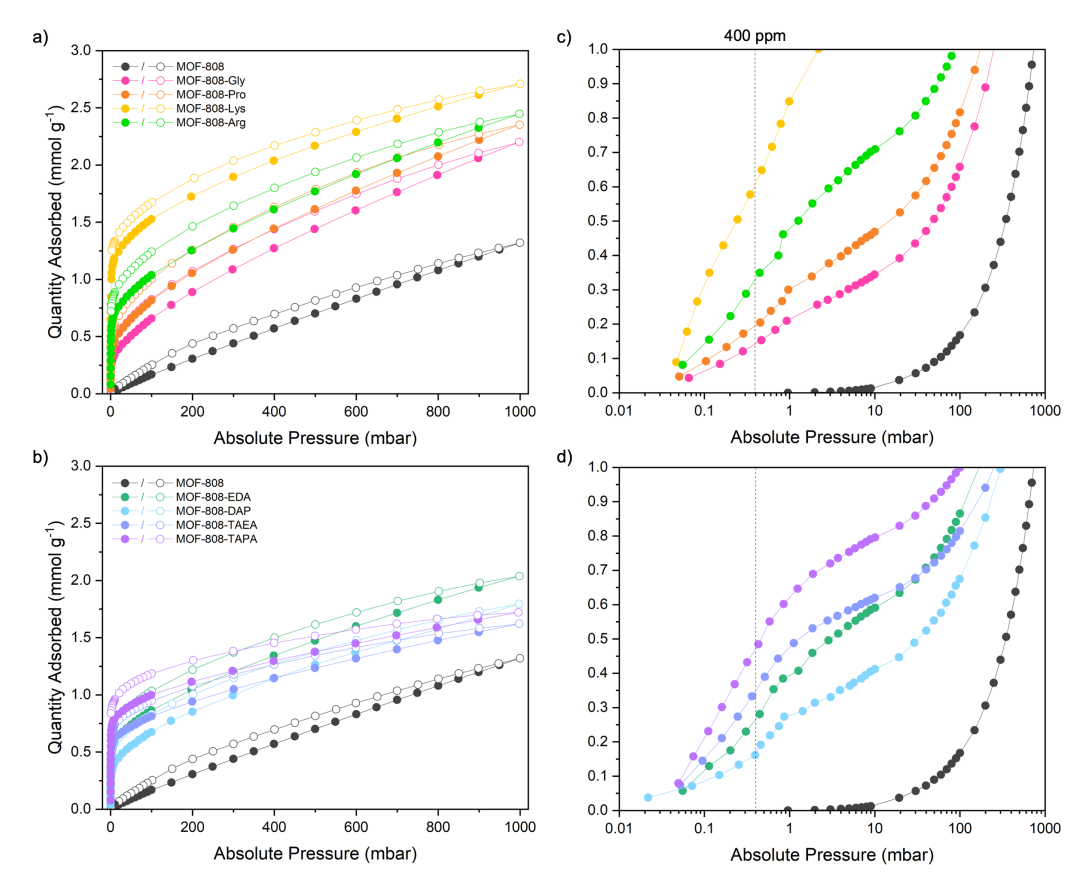


Figure 4. Comparison of CO₂ sorption isotherms measured at 25 °C for (a) MOF-808 and the MOF-808-AA series and (b) MOF-808 and the MOF-808-PA series with pressure plotted on a linear scale and a logarithmic scale (c)(d) to highlight the uptake at the DAC-relevant pressure.

Carbon dioxide sorption analysis

To evaluate the CO₂ adsorption capacity at a concentration of 400 ppm, which approximates atmospheric CO₂ levels, dry CO₂ sorption isotherms were measured for all variants of MOF-808 as well as the pristine MOF-808 at 298 K (Figure 4a, Section S9). Despite having the highest BET surface area among all the candidates, MOF-808 exhibited the lowest CO₂ uptake across the entire pressure range from 0 to 1000 mbar, which suggests a lack of strong adsorption sites for CO2 molecules within MOF-808. In contrast, all amine-functionalized MOF-808 variants displayed significantly enhanced CO₂ uptakes even though they featured lower porosity compared to the pristine framework. Within the MOF-808-AA series (Figure 4a), namely MOF-808-Gly, MOF-808-Pro, and MOF-808-Arg, they demonstrated the ability to adsorb CO₂ within the range of 0.142 to 0.342 mmol g⁻¹ at this DAC relevant CO₂ concentration. Particularly noteworthy is MOF-808-Lys, which displayed an uptake of 0.612 mmol g⁻¹, the highest among all functionalized MOF-808 sorbents. This increased CO₂ adsorption can be credited to the highly reactive amine groups within the pores, providing strong chemisorption sites for CO₂ molecules. Furthermore, the quantity of CO₂ captured was influenced by a combination of factors, including the effective gravimetric loading, basicity, and accessibility of these amine species. In the cases of MOF-808-Lys and MOF-808-Arg, their high pK_a values and substantial gravimetric loading of amines created environments with more reactive and densely packed sorption sites for CO2, resulting in higher uptake compared to MOF-808-Gly and MOF-808-Pro. The disparity in uptake between MOF-808-Lys and MOF-808-Arg can be attributed to the lower pore accessibility of the latter, which was due to greater steric hindrance resulting from the larger molecular size of L-arginine and incomplete removal of residual ethylene glycol molecules within the pores (Figure S6). In summary, among the studied variants, MOF-808-Lys demonstrated the highest CO₂ uptake, showcasing its superior performance in this regard.

In the MOF-808-PA series (Figure 4b), the CO₂ uptakes at 400 ppm ranged from 0.175 mmol g⁻¹ for MOF-808-DAP to 0.498 mmol g⁻¹ for MOF-808-TAPA, also exhibiting the significant increase in CO₂ uptake compared to pristine MOF-808 due to the two-step polyamine installation. MOF-808-TAPA stood out with the highest gravimetric amine loading, consequently yielding the highest CO₂ capture performance. Furthermore, despite both being functionalized with diamine species, MOF-808-EDA presented a slightly higher CO₂ uptake than MOF-808-DAP, which featured the street 3-carbon 1,3-diaminopropane. This observation sugget amount of CO₂ adsorbed is influenced not only by basicity but also by the quantity of amine loading. It is important to highlight that the CO₂ sorption performance of the MOF-808-PA series differed notably from that of the MOF-808-AA series at high pressure ranges of CO₂. Typically, the variants in the MOF-808-AA series exhibited higher uptakes in the highpressure range compared to the MOF-808-PA series. This phenomenon was likely attributed to the generally lower BET

surface areas of the MOF-808-PA samples, resulting in reduced physisorption of CO_2 . The CO_2 isotherm measurements demonstrated that MOF-808 serves as a robust platform for basic amine functionalization, offering promising chemisorption sites for strong CO_2 interaction, even at relatively low CO_2 partial pressures, which is advantageous for DAC applications.

Dynamic breakthrough measurements

To further assess the CO_2 capture performance in the context of practical DAC applications, dynamic breakthrough measurements were conducted (Figure 5, Section S10), which is essential since most capturing scenarios involve high gas flow rates and the presence of water. MOF-808-Lys and MOF-808-TAPA were once again chosen to measure CO_2 uptakes under varying RH levels from 0 to 50% to investigate the impact of water vapor. The samples were activated within the reaction column, and the desired gas feed, containing 400 ppm of CO_2 with different humidity levels, was precisely controlled by adjusting the blend ratio of humidified and dry compressed air. The CO_2 uptakes were calculated through numerical integration of the monitored outlet concentrations of CO_2 .

With breakthrough measurement, MOF-808-Lys (Figure 5a) showed a CO_2 uptake of 0.556 mmol g^{-1} at dry condition, which represented a 9% decrease when compared to its single-component CO_2 isotherm. This decline can likely be assigned to the slow kinetics of the interaction between MOF-808 and CO_2 , a phenomenon that was also evident during extended isotherm measurements. By introducing 10% RH, the adsorption capacity can be increased to 0.613 mmol g^{-1} .

Furthermore, the uptake increased to 0.865 mmol g⁻¹ in the presence of 25% RH as a 56% enhancement compared to its dry breakthrough uptake. Notably, by doubling the RH to 50%, an exceptional boost in CO₂ uptake to 1.205 mmol g⁻¹ was observed, representing a remarkable 2.17-fold increase over the dry breakthrough uptake and a 1.97-fold increase over the single-component isotherm. This experiment effectively demonstrated that under varying humidity conditions, moisture can significantly enhance the adsorption efficiency of CO₂ to varying degrees. In the case of MOF-808-TAPA (Figure 5b), the CO₂ uptake reached 0.454 mmol g⁻¹ under dry conditions, which similarly indicates a 9% deviation from the uptake observed in the dry isotherm. The CO2 uptake increased to 0.757 mmol g-1 in the presence of 10% RH, translating to a 67% enhancement. Elevating the humidity to 25% did not yield a significant increase, resulting in only a slightly higher uptake of 0.796 mmol g⁻¹. Finally, employing a 50% RH condition allowed for an uptake of 0.872 mmol g⁻¹, marking a 75% increase in comparison to the uptake observed in the dry isotherm. Interestingly, the breakthrough sorption behavior of MOF-808-TAPA differed from that of MOF-808-Lys, as the increase in outlet CO₂ concentration was much slower in the presence of 10% and 25% RH. However, the rate at which the outlet CO₂ concentration increased as adsorption approached saturation largely accelerated with 50% RH, suggesting that water enhance the kinetics of CO₂ uptake of MOF-808-TAPA at high humidity conditions.

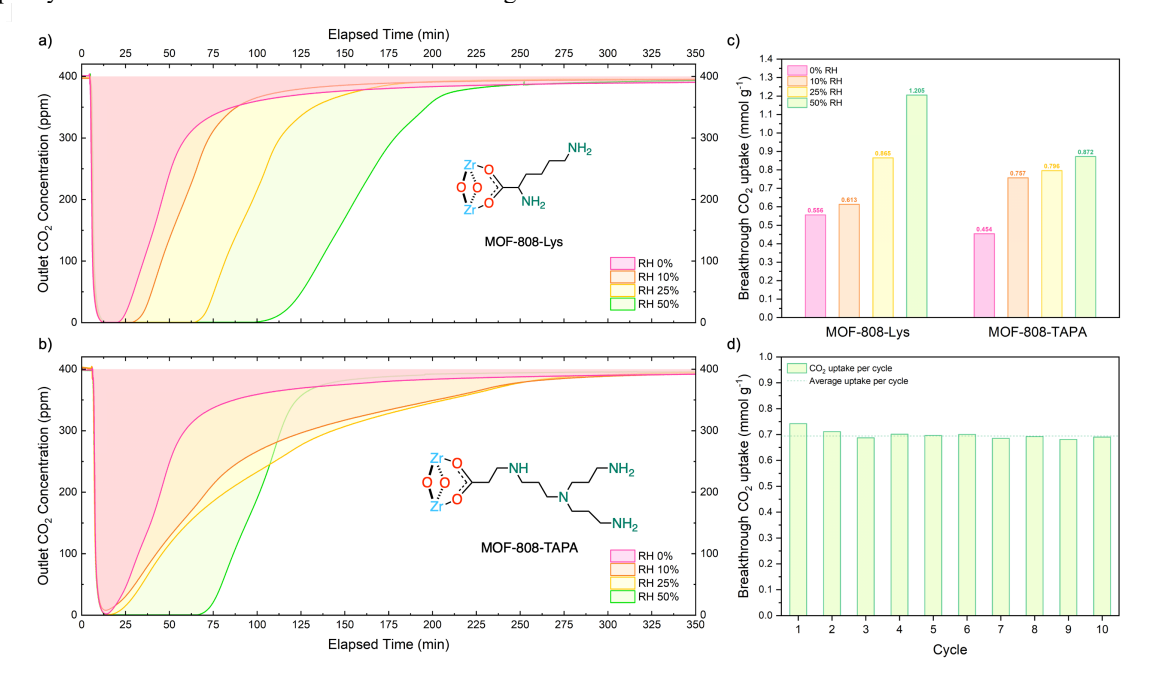


Figure 5. Dynamic breakthrough measurements at 25 °C with 0%, 10%, 25%, and 50% RH for (a) MOF-808-Lys and (b) MOF-808-TAPA. In the plot of the outlet CO_2 concentration, the CO_2 uptake can be derived through numerical integration of the marked area. (c) Comparison of CO_2 uptakes of MOF-808-Lys and MOF-808-TAPA by dynamic breakthrough measurements. (d) CO_2 uptakes of MOF-808-Lys at 400 ppm, 50% RH derived from the temperature-swing cycling measurement. The average working capacity was 0.696 mmol g^{-1} cycle⁻¹.

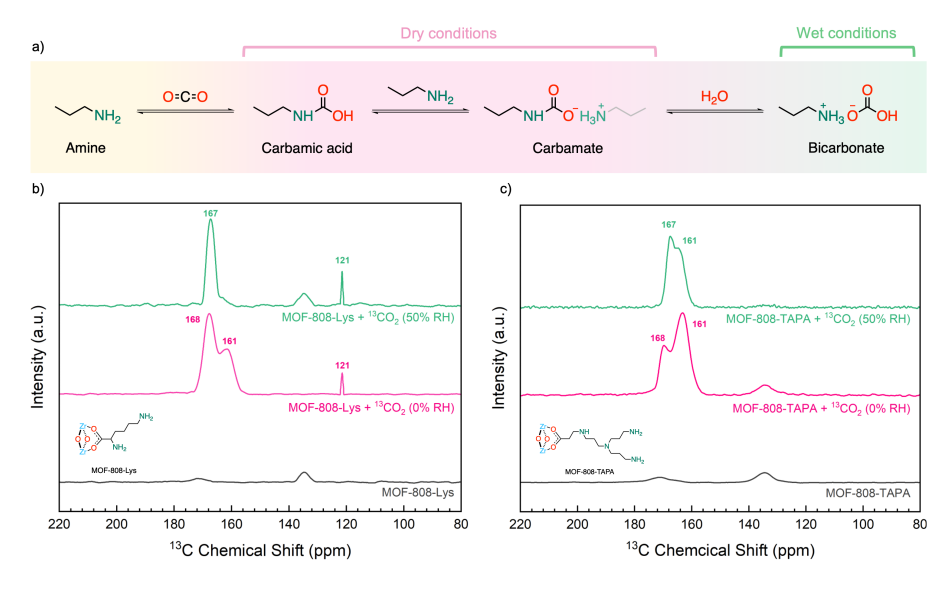


Figure 6. (a) Chemisorption mechanism of amines and CO_2 in dry conditions and in the presence of water. ^{13}C solid-state NMR spectra on (b) MOF-808-Lys and (c) MOF-808-TAPA. Bottom: pristine MOF samples; middle: $^{13}CO_2$ dosing under dry conditions; top: $^{13}CO_2$ dosing with 50% RH.

Given the remarkable CO₂ uptake in humid conditions, a temperature-swing cycling test (Figure 5c, Section S11) was conducted on MOF-808-Lys at DAC condition (400 ppm CO₂ with 50% RH). For the measurement efficiency, a quick scan process was employed: both the sorption measurement and the regeneration process were set to conclude when the outlet CO₂ concentration reached 380 ppm and 20 ppm, respectively. While this approach resulted in some partial CO₂ uptake loss, it still allowed for the evaluation of the reproducibility of sorption-desorption behavior. The measured uptake capacity was determined to be 0.696 mmol g⁻¹ cycle⁻¹ over ten consecutive cycles without significant decay.

Solid-state NMR study

To examine the sorption characteristics of amine-functionalized MOF-808, solid-state cross-polarization magic-angle spinning (CP-MAS) ¹³C NMR spectra were measured for MOF-808-Lys, and MOF-808-TAPA (Figure 6). This analysis aimed to assess alterations in the chemical composition before and after the introduction of ¹³CO₂, in the presence and absence of water. Hence, the solid-state NMR spectra of these samples were measured under three distinct conditions: (1) activated samples, (2) adsorption of CO₂ under dry condition, and (3) adsorption of CO₂ with 50% RH.

In the ¹³C NMR spectra, weak signals at 172 and 134 ppm were observed in both MOF variants before and after CO₂ sorption, which correspond to the carboxylate and aromatic carbons of the MOF linkers. Both MOF variants were exposed to ¹³CO₂ under dry conditions and at 50% RH at 298 K for 24 hours. In both samples, two distinct signals at 161 and 168 ppm appeared after loading ¹³CO₂ under dry conditions, indicating the formation of carbamic acid or carbamate^{28, 29} through covalent interaction between ¹³CO₂ and primary amine moieties. For the wet conditions, notably, MOF-808-Lys exhibited a single signal at 167 ppm under 50% RH (Figure 6b), attributed to ammonium bicarbonate formation^{28, 29}. The presence of water enhanced amine utilization efficiency through the formation of bicarbonate species, resulting in increased CO₂ uptake compared to the dry conditions. Conversely, MOF-808-TAPA presented two signals under humid

conditions (Figure 6c), possibly due to incomplete conversion from carbamic acid/carbamate to bicarbonate. This discrepancy in conversion may be linked to the higher water uptake by MOF-808-Lys (~0.17 g g⁻¹) compared to MOF-808-TAPA (~0.09 g g⁻¹) at 50% RH. The incomplete conversion of bicarbonate in MOF-808-TAPA led to a lower increase in CO₂ uptake by water vapor compared to MOF-808-Lys during the dynamic breakthrough measurement. Furthermore, a signal at 121 ppm was observed in the MOF-808-Lys sample, both with and without the presence of water. This signal was ascribed to physiosorbed ¹³CO₂. In contrast, free ¹³CO₂ was not detected in the MOF-808-TAPA sample. Due to the presence of functionalized branched amines, the BET surface area of MOF-808-TAPA (321 m² g⁻¹) was lower than half that of MOF-808-Lys (701 m² g⁻¹), which made it challenging for MOF-808-TAPA to accommodate more CO₂ molecules within its pores. This phenomenon provided an explanation for the observed lower CO2 uptakes in the high-pressure ranges of the MOF-808-PA series when compared to the MOF-808-AA series in the context of single-component CO₂ isotherms.

Conclusions

We employed two distinct amine-functionalization strategies for MOF-808, utilizing amino acids that are directly bound to the zirconium SBU, and polyamine incorporation via a two-step nucleophilic substitution. The resulting compounds demonstrated exceptional CO₂ capture capacity and stability when exposed to ambient air containing water vapor. The quantity of loaded amine species, the sorption behavior, and the sorption chemistry have been fully characterized. This research showcased the extensive tunability of MOF-808 and unveiled substantial potential for amine-functionalization in the development of solid-state sorbents for DAC relative applications.

ASSOCIATED CONTENT

Supporting Information

The Supporting Information is available free of charge on the ACS Publications website.

Detailed experimental procedures, synthesis and characterization details of the reported compounds, including digest NMR, Potentiometric acid-base titration, PXRD, SEM-EDS analysis, nitrogen sorption isotherms, water vapor sorption isotherms, CO₂ sorption isotherms, dynamic breakthrough measurements, and solid-state NMR (PDF)

AUTHOR INFORMATION

Corresponding Author

Omar M. Yaghi – Department of Chemistry and Kavli Energy Nanoscience Institute, University of California, Berkeley, California 94720, United States; Bakar Institute of Digital Materials for the Planet, College of Computing, Data Science, and Society, University of California, Berkeley, California 94720, United States; KACST–UC Berkeley Center of Excellence for Nanomaterials for Clean Energy Applications, King Abdulaziz City for Science and Technology, Riyadh 11442, Saudi Arabia Email: yaghi@berkeley.edu

Authors

Oscar Iu-Fan Chen – Department of Chemistry and Kavli Energy Nanoscience Institute, University of California, Berkeley, California 94720, United States; Bakar Institute of Digital Materials for the Planet, College of Computing, Data Science, and Society, University of California, Berkeley, California 94720, United States. ORCID ID: orcid.org/0000-0003-4361-0768

Cheng-Hsin Liu – Department of Chemistry and Kavli Energy Nanoscience Institute, University of California, Berkeley, California 94720, United States; Bakar Institute of Digital Materials for the Planet, College of Computing, Data Science, and Society, University of California, Berkeley, California 94720, United States

Kaiyu Wang – Department of Chemistry and Kavli Energy Nanoscience Institute, University of California, Berkeley, California 94720, United States; Bakar Institute of Digital Materials for the Planet, College of Computing, Data Science, and Society, University of California, Berkeley, California 94720, United States.

Haozhe Li – Department of Chemistry and Kavli Energy Nanoscience Institute, University of California, Berkeley, California 94720, United States; Bakar Institute of Digital Materials for the Planet, College of Computing, Data Science, and Society, University of California, Berkeley, California 94720, United States.

Ali H. Alawadhi – Department of Chemistry and Kavli Energy Nanoscience Institute, University of California, Berkeley, California 94720, United States; Bakar Institute of Digital Materials for the Planet, College of Computing, Data Science, and Society, University of California, Berkeley, California 94720, United States. ORCID ID: orcid.org/0000-0003-2680-5221

ACKNOWLEDGMENT

This work is financially supported by the Department of Energy under Award DE-FE0031956. We thank Ephraim Neumann from the Yaghi research group for his help with SEM-EDS measurement. We thank Zihui Zhou from the Yaghi research group for helpful discussions with material characterizations. We thank Dr. Mark D. Doherty, Dr. David R. Moore, and their colleagues at GE Research for insightful discussions regarding material synthesis and characterizations. We thank Dr. Hasan Celik and UC Berkeley's NMR facility in the College of Chemistry (CoCNMR) for spectroscopic assistance. O.I.-F.C. acknowledges financial support from the Taiwan Ministry of Education.

REFERENCES

- 1. IPCC, 2023: Summary for Policymakers. In: Climate Change 2023: Synthesis Report. Contribution of Working Groups I, II and III to the Sixth Assessment Report of the Intergovernmental Panel on Climate Change. 2023.
- Sanz-Pérez, E. S.; Murdock, C. R.; Didas, S. A.; Jones, C. W., Direct Capture of CO₂ from Ambient Air. Chem. Rev. 2016, 116, 11840-11876.
- Zhu, X.; Xie, W.; Wu, J.; Miao, Y.; Xiang, C.; Chen, C.; Ge, B.; Gan, Z.; Yang, F.; Zhang, M.; O'Hare, D.; Li, J.; Ge, T.; Wang, R., Recent Advances in Direct Air Capture by Adsorption. Chem. Soc. Rev. 2022, 51, 6574-6651.
- IEA, Direct air capture 2022: https://www.iea.org/reports/direct-air-capture-2022 (accessed Oct. 30, 2023).
- Su, F.; Lu, C.; Kuo, S.-C.; Zeng, W., Adsorption of CO₂ on Amine-Functionalized Y-type Zeolites. *Energ. Fuel.* 2010, 24, 1441-1448.
- Bollini, P.; Didas, S. A.; Jones, C. W., Amine-oxide Hybrid Materials for Acid Gas Separations. *J. Mater. Chem.* 2011, 21, 15100-15120
- Lin, Y.; Kong, C.; Chen, L., Amine-Functionalized metal-organic frameworks: structure, synthesis and applications. RSC Adv. 2016, 6, 32598-32614.
- 8. Varghese, A. M.; Karanikolos, G. N., CO₂ Capture Adsorbents Functionalized by Amine–Bearing Polymers: A Review. *Int. J. Greenh. Gas. Con.* **2020**, *96*, 103005.
- 9. Lyu, H.; Li, H.; Hanikel, N.; Wang, K.; Yaghi, O. M., Covalent Organic Frameworks for Carbon Dioxide Capture from Air. *J. Am. Chem. Soc.* **2022**, *144*, 12989-12995.
- Fan, Y.; Jia, X., Progress in Amine-Functionalized Silica for CO₂ Capture: Important Roles of Support and Amine Structure. Energ. Fuel. 2022, 36, 1252-1270.
- Sanz, R.; Calleja, G.; Arencibia, A.; Sanz-Pérez, E. S., Development of High Efficiency Adsorbents for CO₂ Capture Based On A Double-Functionalization Method of Grafting and Impregnation. *J. Mater. Chem. A* 2013, 1, 1956-1962.
- 12. Rochelle, G. T., Amine Scrubbing for CO₂ Capture. *Science* **2009**, *325*, 1652-4.
- Kiani, A.; Jiang, K.; Feron, P., Techno-Economic Assessment for CO₂ Capture from Air Using a Conventional Liquid-Based Absorption Process. Front. Energy Res. 2020, 8, 92.
- Kumar, A.; Madden, D. G.; Lusi, M.; Chen, K. J.; Daniels, E. A.; Curtin, T.; Perry, J. J. t.; Zaworotko, M. J., Direct Air Capture of CO₂ by Physisorbent Materials. *Angew. Chem. Int. Ed. Engl.* 2015, 54, 14372-7.
- Lu, W.; Sculley, J. P.; Yuan, D.; Krishna, R.; Zhou, H.-C., Carbon Dioxide Capture from Air Using Amine-Grafted Porous Polymer Networks. J. Phys. Chem. C 2013, 117, 4057-4061.
- Sujan, A. R.; Pang, S. H.; Zhu, G.; Jones, C. W.; Lively, R. P., Direct CO₂ Capture from Air Using Poly(Ethylenimine)-Loaded Polymer/Silica Fiber Sorbents. ACS Sustain. Chem. Eng. 2019, 7, 5264-5273.
- Cherevotan, A.; Raj, J.; Peter, S. C., An Overview of Porous Silica Immobilized Amines for Direct Air CO₂ Capture. *J. Mater. Chem. A* 2021, 9, 27271-27303.
- Anyanwu, J.-T.; Wang, Y.; Yang, R. T., CO₂ Capture (Including Direct Air Capture) and Natural Gas Desulfurization of Amine-Grafted Hierarchical Bimodal Silica. *Chem. Eng. J.* 2022, 427, 131561.
- Anyanwu, J.-T.; Wang, Y.; Yang, R. T., Amine-Grafted Silica Gels for CO₂ Capture Including Direct Air Capture. *Ind. Eng. Chem. Res.* 2019, 59, 7072-7079.
- Sumida, K.; Rogow, D. L.; Mason, J. A.; McDonald, T. M.; Bloch, E. D.; Herm, Z. R.; Bae, T. H.; Long, J. R., Carbon Dioxide Capture in Metal-Organic Frameworks. *Chem. Rev.* 2012, 112, 724-81.
- McDonald, T. M.; Lee, W. R.; Mason, J. A.; Wiers, B. M.; Hong, C. S.; Long, J. R., Capture of Carbon Dioxide From Air and Flue Gas in The Alkylamine-Appended Metal-Organic

- Framework mmen-Mg₂ (dobpdc). J. Am. Chem. Soc. **2012**, 134, 7056-7065.
- Lee, W. R.; Hwang, S. Y.; Ryu, D. W.; Lim, K. S.; Han, S. S.; Moon, D.; Choi, J.; Hong, C. S., Diamine-Functionalized Metal-Organic Framework: Exceptionally High CO₂ Capacities from Ambient Air and Flue Gas, Ultrafast CO₂ Uptake Rate, and Adsorption Mechanism. *Energ. Environ. Sci.* 2014, 7, 744-751.
- Shekhah, O.; Belmabkhout, Y.; Chen, Z.; Guillerm, V.; Cairns, A.; Adil, K.; Eddaoudi, M., Made-To-Order Metal-Organic Frameworks for Trace Carbon Dioxide Removal and Air Capture. *Nat. Comm.* 2014, 5, 4228.
- Bien, C. E.; Chen, K. K.; Chien, S.-C.; Reiner, B. R.; Lin, L.-C.; Wade, C. R.; Ho, W. W., Bioinspired Metal-Organic Framework for Trace CO₂ Capture. J. Am. Chem. Soc. 2018, 140, 12662-12666.
- Sadiq, M. M.; Batten, M. P.; Mulet, X.; Freeman, C.; Konstas, K.; Mardel, J. I.; Tanner, J.; Ng, D.; Wang, X.; Howard, S., A Pilot-Scale Demonstration of Mobile Direct Air Capture Using Metal-Organic Frameworks. Adv. Sustainable Syst. 2020, 4, 2000101
- Darunte, L. A.; Oetomo, A. D.; Walton, K. S.; Sholl, D. S.; Jones, C. W., Direct Air Capture of CO₂ Using Amine Functionalized MIL-101 (Cr). ACS Sustain. Chem. Eng. 2016, 4, 5761-5768.
- Zeng, Y.; Zou, R.; Zhao, Y., Covalent Organic Frameworks for CO2 Capture. Adv. Mater. 2016, 28 (15), 2855-73.
- Lyu, H.; Chen, O. I.-F.; Hanikel, N.; Hossain, M. I.; Flaig, R. W.; Pei, X.; Amin, A.; Doherty, M. D.; Impastato, R. K.; Glover, T. G., Carbon Dioxide Capture Chemistry of Amino Acid Functionalized Metal-Organic Frameworks in Humid Flue Gas. J. Am. Chem. Soc. 2022, 144, 2387-2396.
- Flaig, R. W.; Osborn Popp, T. M.; Fracaroli, A. M.; Kapustin, E. A.; Kalmutzki, M. J.; Altamimi, R. M.; Fathieh, F.; Reimer, J. A.; Yaghi, O. M., The Chemistry of CO₂ Capture in An Amine-Functionalized Metal-Organic Framework Under Dry and Humid Conditions. J. Am. Chem. Soc. 2017, 139, 12125-12128.
- Furukawa, H.; Gándara, F.; Zhang, Y.-B.; Jiang, J.; Queen, W. L.; Hudson, M. R.; Yaghi, O. M., Water Adsorption in Porous Metal–Organic Frameworks and Related Materials. *J. Am. Chem. Soc.* 2014, *136*, 4369-4381.
- Baek, J.; Rungtaweevoranit, B.; Pei, X.; Park, M.; Fakra, S. C.; Liu, Y.-S.; Matheu, R.; Alshmimri, S. A.; Alshehri, S.; Trickett, C. A., Bioinspired Metal–Organic Framework Catalysts for Selective Methane Oxidation to Methanol. *J. Am. Chem. Soc.* 2018, 140, 18208-18216.
- Hu, Z.; Kundu, T.; Wang, Y.; Sun, Y.; Zeng, K.; Zhao, D., Modulated Hydrothermal Synthesis of Highly Stable MOF-808 (Hf) for Methane Storage. ACS Sustain. Chem. Eng. 2020, 8, 17042-17053.
- Jiang, J.; Gándara, F.; Zhang, Y.-B.; Na, K.; Yaghi, O. M.; Klemperer, W. G., Superacidity in Sulfated Metal–Organic Framework-808. J. Am. Chem. Soc. 2014, 136, 12844-12847.
- Mautschke, H.-H.; Drache, F.; Senkovska, I.; Kaskel, S.; i Xamena, F. L., Catalytic Properties of Pristine and Defect-Engineered Zr-MOF-808 Metal Organic Frameworks. *Catal. Sci. Technol.* 2018, 8, 3610-3616.
- Zhang, W.; Bu, A.; Ji, Q.; Min, L.; Zhao, S.; Wang, Y.; Chen, J., pK_a-Directed Incorporation of Phosphonates into MOF-808 via Ligand Exchange: Stability and Adsorption Properties for Uranium. ACS Appl. Mater. Inter. 2019, 11, 33931-33940.
- Aunan, E.; Affolter, C. W.; Olsbye, U.; Lillerud, K. P., Modulation of the Thermochemical Stability and Adsorptive Properties of MOF-808 by the Selection of Non-structural Ligands. *Chem. Mater.* 2021, 33, 1471-1476.
- Ji, C.; Ren, Y.; Yu, H.; Hua, M.; Lv, L.; Zhang, W., Highly Efficient and Selective Hg (II) Removal from Water by Thiol-Functionalized MOF-808: Kinetic and Mechanism Study. Chem. Eng. J. 2022, 430, 132960.
- 38. Weast, R. C., CRC Handbook of Chemistry and Physics. A ready-reference book of chemical and physical data. 1975.

- Klet, R. C.; Liu, Y.; Wang, T. C.; Hupp, J. T.; Farha, O. K., Evaluation of Brønsted Acidity and Proton Topology in Zr-and Hf-Based Metal-Organic Frameworks Using Potentiometric Acid-Base Titration. J. Mater. Chem. A 2016, 4, 1479-1485.
- Yurdakal, S.; Garlisi, C.; Özcan, L.; Bellardita, M.; Palmisano, G., (Photo) Catalyst Characterization Techniques: Adsorption Isotherms and BET, SEM, FTIR, UV-Vis, Photoluminescence, and Electrochemical Characterizations. *In Heterogeneous Photocatalysis*, Elsevier 2019, 87-152.

Insert Table of Contents artwork here

